

A Multi-Lead Fusion Method for the Accurate Delineation of QRS Complex Location in 12 Lead ECG Signal

Chhaviraj Chauhan, *Research Scholar, Bharti School, IIT, Delhi,*

Monika Agrawal, *Professor, CARE, IIT Delhi, New Delhi and*

Pooja Shabherwal, *Assistant Professor, The NorthCap University, Gurgaon*

Abstract

This paper presents a multi-lead fusion method for the accurate and automated detection of the QRS complex location in 12 lead ECG (Electrocardiogram) signals. The proposed multi-lead fusion method accurately delineates the QRS complex by the fusion of detected QRS complexes of the individual 12 leads. The proposed algorithm consists of two major stages. Firstly, the QRS complex location of each lead is detected by the single lead QRS detection algorithm. Secondly, the multi-lead fusion algorithm combines the information of the QRS complex locations obtained in each of the 12 leads. The performance of the proposed algorithm is improved in terms of Sensitivity and Positive Predictivity by discarding the false positives. The proposed method is validated on the ECG signals with various artifacts, inter and intra subject variations. The performance of the proposed method is validated on the long duration recorded ECG signals of St. Petersburg INCART database [1] with Sensitivity of 99.87% and Positive Predictivity of 99.96% and on the short duration recorded ECG signals of CSE (Common Standards for Electrocardiography) multilead database [2] with 100% Sensitivity and 99.13% Positive Predictivity.

Index Terms

12 lead ECG Signal, QRS Complex detection, Multi-lead Fusion, QRS detector,

The manuscript is under review. (corresponding author email address-chhavirajchauhan@gmail.com)

I. INTRODUCTION

EARLY detection of heart diseases have become extremely important as cardiovascular disease (CVDs) are the major cause of mortality worldwide. The ECG signal is an effective non-invasive way for heart rate monitoring in a simple setting, operation room and even for the diagnosis of various heart diseases. The ECG signal is a record of electrical activity of the heart and the 12 lead ECG signal captures the electrical potential of heart from different angles. The 12 lead ECG signal shows the pathological status of cardiovascular system by changes in its waveforms or rhythms [3]. In the clinical environment, physicians analyze the ECG records of patients to judge whether they have a benign or unkind heart state [4]. Manual analysis process is much laborious and repetitive. Hence, automated ECG signal analysis is required. In the past several decades, a plethora of research work has been published on the automatic diagnosis of the cardiovascular diseases.

For automated ECG signal analysis algorithms, the detection of QRS complexes is the first and foremost step, as it corresponds to the electrical excitation of the two ventricles. The duration, morphology and amplitude of the QRS complex provides the information about the current state of the heart. The accurate detection of the QRS complex is an essential step in the automated 12 lead ECG signal analysis, as any cardiac disorder changes the morphology of the QRS complex and the duration of the RR interval, which is considered clinically important. The precise detection of other sub waves like P wave, T wave and ST segment is dependent on the accurate detection of the QRS complex [5].

In literature several methods have been proposed for detection of QRS complex in the ECG signal. Although most of the research groups have worked for detection of QRS complex detection in single lead [6], [7], [8], [9], [10], [11], [12], [13] or two lead [14], [15] ECG signal. To have more precise analysis of the state of the heart, the QRS complex has to be accurately delineated in the 12 lead ECG signal, clinically. For detection of QRS complex in 12 lead ECG signals, the researchers have detected the QRS complex in single lead and then combined them using various combining methods. The popular single lead QRS detection methods used by many authors are Pan-Tompkins method [16], [17], [18], [19], [20], wavelet-based [21], [22], Hilbert transform-based [19] and SVM based [23] algorithms. For the detection of QRS complex in the 12 lead ECG signal, combining or merging methods like voting fusion [17], [18], [20], [22], optimum data fusion [19], OR/AND [20], reliability index [21], combined

entropy [23], complex pan-tompkins wavelet [24] and multi-lead QRS detection algorithm [16] are used by researchers.

In [16], the QRS complex is detected on single lead by using Pan-Tomkins algorithm and then multi-lead detection algorithm is used for delineation of QRS complex on the 15 Lead ECG signal. In this work, 12 standard lead and 3 orthogonal leads XYZ were used for the evaluation. For a valid QRS detection, all 15 QRS location of each lead is required. Therefore, this method can only reduce the false QRS detection with a reduction of true QRS detection. This algorithm was evaluated on CSE(Common Standards for Electrocardiography) multilead database [2], [25] having short duration ECG records, only in terms of mean and standard deviations but the sensitivity and positive predictivity is not presented. In [26], the QRS complex was detected on the 12 lead ECG signal but the detection on each lead was done sequentially. In [23] Mehta et al. presented a support vector machine based 12 lead QRS detector and validated the algorithm on CSE database only. The performance of the algorithm was not evaluated on any long time recorded ECG signals as in INCART database. Saini et al. [27] presented a KNN based method and evaluated on CSE database but the results for single lead ECG signal are only presented.

In a work done by Ledezma et al. [19], six different single lead QRS detector and optimum data fusion algorithm was used and evaluated on INCART database with good sensitivity but a supervised training period of few minutes was required for the calculation of weight coefficients associated with each lead. The work reported by Mondelo et al. [28] detected the QRS complex location by arranging all available QRS complex location in ascending order and then by defining two limits. The method first detects the actual QRS locations and later the false positives, which make the algorithm not suitable for real medical applications. In the work presented by Huang et al. [29], the Principal Component Analysis and the Combined Wavelet Entropy were used to detect QRS complex location but the method is not possible in real time application, as the full ECG signal recording is required to extract the principal components. In a recent work done by Thurner et al. [24], three single lead algorithms was merged and the multilead ECG signal was reduced to single ECG signal by averaging it. So it became a single lead QRS detection algorithm. However, many researchers presented various algorithms but still there are gaps to detect QRS complex accurately due to several reasons including diversity of the QRS waveform, low signal-to noise ratio (SNR), inter and intra morphological changes and artifacts accompanying ECG

signals. Many of the existing algorithms are also not able to perform noise reduction and QRS complex detection simultaneously for the 12 lead ECG signal.

In this paper, an efficient multi-leads fusion algorithm is presented for the delineation of QRS complex in the 12 lead ECG signal. The QRS complex is detected in each lead of the observed 12 lead ECG signal using combination of wavelet transform, Hilbert transform and adaptive thresholding [10]. The detected QRS complexes in all the 12 lead are fused together by the proposed multi-leads fusion method to have accurate delineation of QRS complex in the 12 lead ECG signal. The method gives average sensitivity and positive predictivity of 99.87% and 99.96% respectively for INCART database [1] and 100% sensitivity and 99.13% positive predictivity for the CSE database [2].

II. PROBLEM FORMULATION

The QRS complex detection is the most important point in analysis of the state of the heart. The QRS complex location is essential for the majority of the automatic arrhythmia detection algorithm. The classification efficiency of any cardiac abnormality detection method from ECG signal is also depends on the QRS complex detection algorithm. The QRS detector with low sensitivity and positive predictivity directly degrade the classification algorithm's performance, which led to a futile ECG analysis system. The sensitivity and positive predictivity of the automatic detectors depends on the accurate detection of QRS complex. Most of the researchers have worked on the single lead ECG signal. But as, the 12 lead ECG signal captures the electrical potential of heart from different angles, which gives more precise information of the status of the heart. Therefore, here the algorithm is proposed, which automatically detects QRS complex on the 12 lead ECG signal. In this algorithm, the QRS complex is detected on each lead and then fused together intelligibly. For detection of QRS complex any single lead detector can be used and then fused together by the proposed fusion method. Here, the single lead detector proposed in [10] is used as it gives better sensitivity and positive predictivity as compared to the other detectors proposed in literature. Before discussing fusion algorithm for 12 lead ECG signals, the single lead QRS complex detection algorithm is summarized ahead.

A. Detection of QRS in single lead

Mathematically, the single lead ECG signal $z[n]$ can be represented as[30].

$$z[n] = s[n] + w[n] \quad (1)$$

where $s[n]$ represents the ECG signal and $w[n]$ represents the artifacts present in the ECG signal. For diagnosis of the disease in the 12 lead ECG signal, the first step is to detect QRS complex location accurately. As the recorded ECG signal is corrupted by various artifacts such as baseline wandering artifact, motion artifacts, and muscles contraction artifacts. These artifacts are to be removed from each lead for accurate delineation of QRS complex from the 12 lead ECG signal.

The initial pre-processing i.e removing of various artifacts is done using discrete wavelet transform (DWT) with db6 mother wavelet. The DWT analyzes the signal at different resolution (hence, multi resolution) through the decomposition of the signal into several successive frequency subbands. The noise content is significant in high frequency detail subbands, while most of the spectral energy lies in low frequency subbands [31]. As the energy spectrum of db6 mother wavelet is concentrated at low frequencies and its shape resembles the QRS complex, therefore it has turned out to be the best choice among other wavelet functions for this problem. [32]. The DWT is performed on the observed ECG signal $z[n]$ by passing it through high pass filter $h[n]$ and a low-pass filter $l[n]$ with a down sampling factor of 2 as in (2) and (3):

$$d_i[n] = \sum_k z[k] \cdot h[2n - k] \quad (2)$$

$$a_i[n] = \sum_k z[k] \cdot l[2n - k] \quad (3)$$

where $i \in I$, $d_i[n]$ and $a_i[n]$ are detail and approximation coefficients. The approximation and detail information obtained till level 10 are labeled as $a_1[n]$ to $a_{10}[n]$ and $d_1[n]$ to $d_{10}[n]$, respectively. As the QRS complex of a ECG signal lies in a frequency band of 5 to 25 Hz [33], the details coefficients d_4 and d_5 are only considered [10] and the estimated ECG signal $s_0[n]$ is obtained as the sum of d_4 and d_5 . To further attenuate the non-QRS region, the reconstructed signal $s_0[n]$ is passed through the following

low pass filter [10].

$$s_{LP}[n] = \frac{1}{8} \sum_{n_0=1}^7 \frac{12}{5} s_0[n - n_0] - \frac{12}{5} s_0[n - n_0 - 2] - \frac{11}{10} s_0[n - n_0 - 4] \quad (4)$$

After low pass filtering, the hilbert transform of the signal $s_{LP}[n]$ is performed to have the envelope of the QRS complex as in (5),

$$s_H[n] = H(s_{LP}[n]) \quad (5)$$

The QRS complex obtained in (5) $s_H[n]$ is further accentuated as $s_{nl}[n]$ by applying non linear transform as,

$$s_{nl}[n] = \frac{1}{|s_H[n]|} s_H^2[n] \quad (6)$$

The enhanced peaks R_{Loc} are accurately delineated by applying adaptive thresholding [10],

$$R_{Loc} = \mathcal{T}_a(s_{nl}[n]) \quad (7)$$

Where R_{Loc} has the locations of detected QRS complex for a single lead ECG signal obtained by adaptive thresholding.

B. Detection of QRS complex in 12 Lead ECG signal

The delineation of QRS complex is done for all the 12 leads by the aforementioned method and the detected QRS complexes for each lead are labeled as:

$$R_{Locl} = [R_l(1), R_l(2), R_l(3) \dots R_l(N_l)] \quad (8)$$

where l denotes the lead index and N_l is the number of detected QRS complex in l^{th} lead. Hence, the detected QRS complexes for L lead ECG signal can be represented as:

$$\begin{bmatrix} R_{Loc1} \\ R_{Loc2} \\ \vdots \\ R_{LocL} \end{bmatrix} = \begin{bmatrix} R_1(1) & R_1(2) & \dots & R_1(N_1) \\ R_2(1) & R_2(2) & \dots & R_2(N_2) \\ \vdots & \vdots & \dots & \vdots \\ R_L(1) & R_L(2) & \dots & R_L(N_L) \end{bmatrix} \quad (9)$$

Here, L is used as the proposed algorithm can give results for any combination of L leads. We have validated our results with $L = 12$. Practically, the number of detected QRS complex may be different for each lead, as the QRS detector might give some false alarm or might miss some points in a particular lead. So, to get a final accurate QRS complex, a fusion algorithm is required which merges the detected QRS complex of each lead belonging to the same cycle and ignores the false detection obtained in each lead.

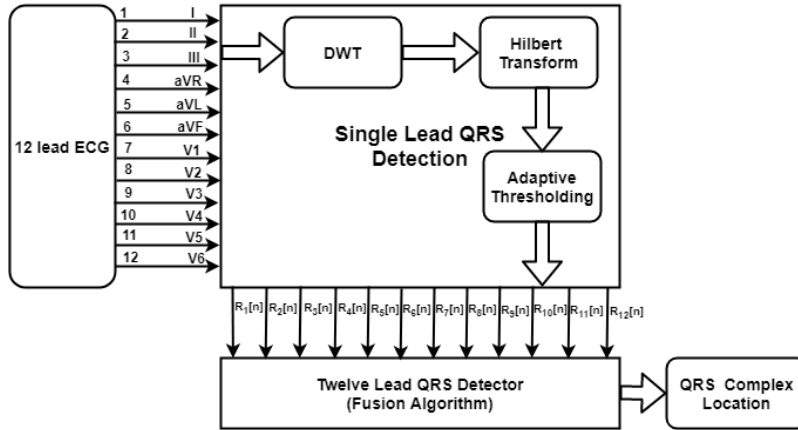


Fig. 1: An overview of 12 lead QRS complex detection method

C. Proposed Fusion method

The QRS complex locations detected in (9) are combined using the proposed fusion method for accurate delineation of QRS complex in the L lead ECG signal. For a better estimate of QRS complex location, the proposed algorithm fuses the detected QRS complex locations corresponding to the same cardiac cycle of each lead. The biggest challenge with this algorithm is to ascertain that the detected QRS complex belong to the same cardiac cycle. As each lead will have its own physiology, and the corresponding QRS complex of particular cardiac cycle in all leads might not be detected at exactly the same sequence. Moreover, while detecting QRS complex there might be some false negatives, or some low amplitude QRS complexes which are missed by algorithm. Therefore a robust algorithm is required for accurate delineation of QRS complex in L lead ECG signal. The algorithm must be able to identify outliers and missed detection, before fusion of detected beats in the L leads. Clinically, physicians also use all nearby QRS complexes

to ascertain the position of the QRS complex corresponding to the given beat. To demonstrate this fact, a fusion algorithm has been suggested for accurate delineation of QRS complex, which is discussed ahead.

Let $R[n] = [R_1(n), R_2(n), R_3(n), \dots, R_L(n)]$, QRS complex vector, be the detected QRS complexes corresponding to the L leads. The $[R_1(n), R_2(n), R_3(n), \dots, R_L(n)]$ in $R[n]$ may correspond to the n th beat.

The first step is to arrange the detected QRS complex vector $R[n]$ in the ascending order as,

$$\mathbf{f}[n] \triangleq \text{sort}(R[n]) = [f_1(n), f_2(n), f_3(n), \dots, f_L(n)] \quad (10)$$

where $\mathbf{f}[n]$ indicates the sorted values of QRS complex. $QRS_{min}[n]$ and $QRS_{max}[n]$ is the minimum and maximum value of the ascended QRS complex sequence $\mathbf{f}[n]$ as,

$$QRS_{min}[n] \triangleq \min(\mathbf{f}[n]) = f_1(n) \quad (11)$$

$$QRS_{max}[n] \triangleq \max(\mathbf{f}[n]) = f_L(n) \quad (12)$$

Two local arrays $\alpha_1[n]$ and $\alpha_2[n]$ are defined as,

$$\alpha_1[n] = \mathbf{f}[n] : f_i[n] \in [QRS_{min}[n], (QRS_{min}[n] + \delta)] \quad 1 \leq i \leq L \quad (13)$$

$$\alpha_2[n] = \mathbf{f}[n] : f_i[n] \in [(QRS_{max}[n] - \delta), QRS_{max}[n]] \quad 1 \leq i \leq L \quad (14)$$

where δ should lie between 80ms to 100ms which is the time span of QRS complex clinically [34]. Therefore a mean value $\delta = 90ms$ is used in this work.

Before proceeding, we are defining few terms for clarity:

- **Equivalent arrays:** The two arrays $\alpha_1[n]$ and $\alpha_2[n]$ are equivalent if their cardinality is equal, i.e.

$$\mathbf{card}(\alpha_1[n]) = u = \mathbf{card}(\alpha_2[n]) = v \quad (15)$$

where u and v are the cardinality of $\alpha_1[n]$ and $\alpha_2[n]$ respectively.

- **Identical arrays:** Further, if two arrays are equivalent i.e. have same cardinality and have same elements than the two arrays $\alpha_1[n]$ and $\alpha_2[n]$ are said to be identical. Mathematically, identical

arrays are defined as:

$$\begin{aligned} \mathbf{card}(\alpha_1[n]) = u = \mathbf{card}(\alpha_2[n]) = v \quad \text{and,} \\ \alpha_1^j[n] = \alpha_2^j[n] \quad \forall j, \quad 1 \leq j \leq u, v \end{aligned} \quad (16)$$

where, j is the index for elements in $\alpha_1[n]$ and $\alpha_2[n]$.

- **Absolutely identical arrays:** The identical arrays with cardinality L are known to be absolutely identical arrays.
- **Equivalent but not identical arrays:** That means, cardinality of both arrays are equal and their elements are not same,

$$\begin{aligned} \mathbf{card}(\alpha_1[n]) = u = \mathbf{card}(\alpha_2[n]) = v \quad \text{and,} \\ \alpha_1^j[n] \neq \alpha_2^j[n] \quad \forall j, \quad 1 \leq j \leq u, v \end{aligned} \quad (17)$$

- **Neither equivalent nor identical arrays:** That means, cardinality of both arrays are not equal and their elements are not same,

$$\begin{aligned} \mathbf{card}(\alpha_1[n]) \neq \mathbf{card}(\alpha_2[n]) \quad \text{and,} \\ \alpha_1^j[n] \neq \alpha_2^j[n] \quad \forall j, \quad 1 \leq j \leq u, v \end{aligned} \quad (18)$$

The two arrays ($\alpha_1[n]$ and $\alpha_2[n]$) generated in (13) and (14) are compared to ascertain that QRS vector $R(n)$ belong to the same cardiac cycle. This leads to the following four cases:

Case 1: Arrays $\alpha_1[n]$ and $\alpha_2[n]$ are absolutely identical: That means the cardinality of both arrays is L and elements of both the arrays are equal. This should imply that all the L detected beats ($R_1[n], R_2[n], R_3[n], \dots, R_L[n]$) are of same cardiac cycle.

Case 2: Arrays $\alpha_1[n]$ and $\alpha_2[n]$ are identical: The cardinality of both arrays is K ($1 \leq K < L$) but less than total number of leads and also elements of both them are equal. This should indicate that the K out of L detected beats belong to the same cardiac cycle.

Case 3: Arrays $\alpha_1[n]$ and $\alpha_2[n]$ are equivalent but not identical: The cardinality of both arrays is K ($1 \leq K < L$) but elements of both them are not equal. This should imply that the K detected beats do not belong to same cardiac cycle.

Case 4: Arrays $\alpha_1[n]$ and $\alpha_2[n]$ are neither equivalent nor identical: The arrays have different cardinality and even the elements of the both arrays are not equal. This should indicate that all the detected beats in QRS complex vector ($R[n]$) do not belong to the same cardiac cycle.

These four cases are discussed ahead in detail,

Case 1: When the generated arrays $\alpha_1[n]$ and $\alpha_2[n]$ are absolutely identical i.e. the cardinality of both the arrays is L and all the entries both the arrays are equal. It deduces that all L detected beats belong to the same cardiac cycle. Hence, all these beats can be combined together to ascertain the correct delineation of QRS complex. The accurate localization of detected QRS complex can be obtained by combining the corresponding beats of all the L leads by some suitable metric like mean, median and mode. Among these statistical parameters, median of the detected beats as defined in (19) is a better measure of central tendency as compared with mode or mean for skewed distributed data [35] as the outliers have a smaller effect on the median.

$$\text{QRS}_{\text{loc}}[n] = \frac{R_{\frac{(L)}{2}}[n] + R_{\frac{(L+2)}{2}}[n]}{2} \quad (19)$$

For better understanding, results corresponding to case 1 for the record I73 of INCART database are depicted in Fig 2. The QRS complex locations detected by the single lead detector are marked on all the 12 leads of the record I73 from INCART database. The arrays $\alpha_1[n]$ and $\alpha_2[n]$ generated for the record are marked in green and red respectively. Since both the arrays are identical, the final estimated QRS complex location is marked, which is very close to the actual QRS complex location with a localization error of 19.46ms only.

Case 2: $\alpha_1[n]$ and $\alpha_2[n]$ are identical i.e. the cardinality of both the arrays is K ($\leq K < L$). It deduces that K detected beats belong to the same cardiac cycle. Hence, all these beats can be combined together to ascertain the correct delineation of QRS complex. The accurate QRS complex location is estimated using (20).

$$\text{QRS}_{\text{loc}}[n] = \begin{cases} R_{\frac{(K+1)}{2}}[n], & \text{if } K \text{ is odd} \\ \frac{R_{\frac{(K)}{2}}[n] + R_{\frac{(K+2)}{2}}[n]}{2}, & \text{if } K \text{ is even} \end{cases} \quad (20)$$

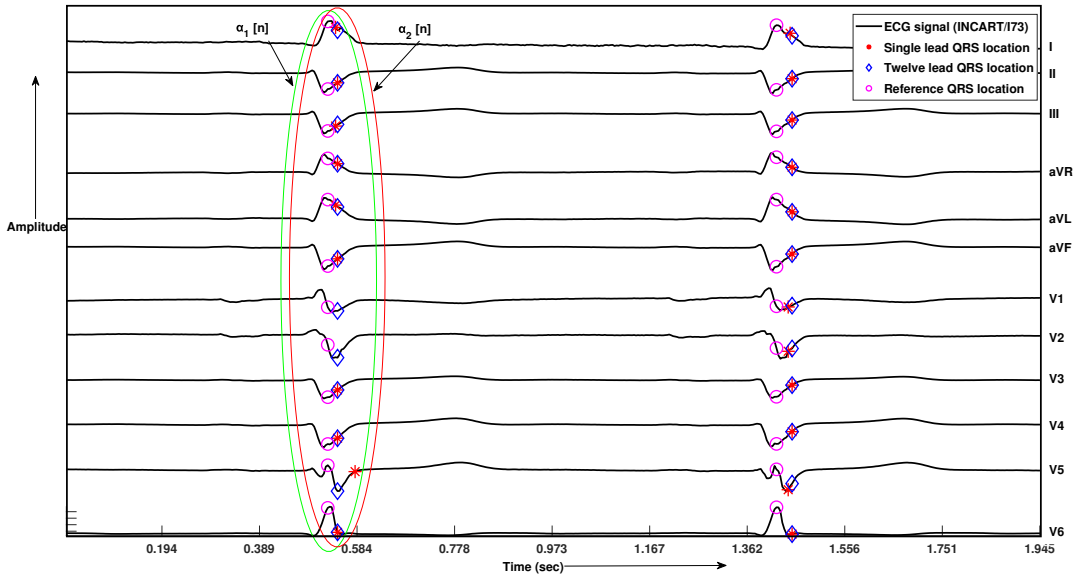


Fig. 2: QRS complex detection by single-lead detector and multi-lead detector in I73 data of INCART database

For this case, the minimum cardinality of both the arrays should be $K \geq 6$. As otherwise if detected beats are < 6 no meaningful fusion is possible. Therefore to ascertain this optimum number of leads required to be combined in the proposed fusion method, an experiment for fusion is conducted for L number of leads ($4 \leq L \leq 11$). The sensitivity and the positive predictivity was observed with varying number of leads. As shown in Fig 3, the sensitivity and positive predictivity increases with a decrease in the number of leads. This is occurring due to increased true positives with increased number of leads. There is an abrupt change in sensitivity and positive predictivity when six leads are used. Beyond this, sensitivity increases, and positive predictivity decreases slightly due to the rise in the false-positive. Hence six leads can be considered as the optimum number for the proposed fusion algorithm.

Case 3: When the cardinality of both arrays $\alpha_1[n]$ and $\alpha_2[n]$ is same but less than L but the entries are not same i.e. temporal locations of these QRS complexes in both arrays are different. The possible reason for this case might be the minimum temporal location $QRS_{min}[n]$ and/or maximum

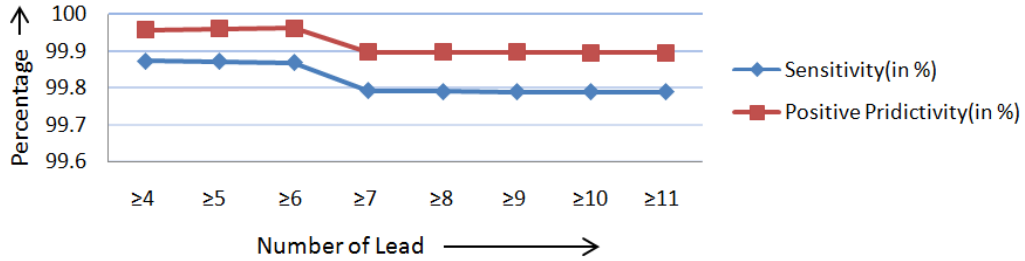


Fig. 3: Performance of proposed method by taking threshold of at least L number of leads

temporal location $QRS_{max}[n]$ are far away from the actual QRS complex location. So for this case, the common entries of both the arrays are systematically extracted. The minimum temporal location of $\alpha_1[n]$ might be due to some false detection so might require replacement with the corresponding next entry and similarly the maximum temporal location of $\alpha_2[n]$ might be either due to miss of the corresponding beat or detection of some other wave e.g. T-wave so should be rejected. The fusion algorithm aims to make both array identical. The accurate QRS location will be detected as in (20), once the array $\alpha_1[n]$ and $\alpha_2[n]$ are identical. The details of the procedure to make these arrays identical is discussed next.

Case 4: When $\alpha_1[n]$ and $\alpha_2[n]$ are not identical, i.e. either the cardinalities of arrays $\alpha_1[n]$ and $\alpha_2[n]$ is not same or the elements of both arrays are not equal. This infers that some false alarms have been detected and they are to discarded by the fusion algorithm. This leads to the following two sub-cases:

$$\text{Case 4(i): } \text{card}(\alpha_1[n]) < \text{card}(\alpha_2[n])$$

$$\text{Case 4(ii): } \text{card}(\alpha_1[n]) > \text{card}(\alpha_2[n])$$

These sub-cases are discussed ahead in detail.

Case 4(i): When cardinality of $\alpha_1[n]$ is less than the cardinality of $\alpha_2[n]$. This implies that the majority of the detected QRS complex locations corresponding to all L leads are close to $QRS_{max}[n]$ and therefore lie in $\alpha_2[n]$. Here, one can infer that the actual QRS complex location is closer to the array $\alpha_2[n]$. Also the minimum temporal location of $\alpha_1[n]$ i.e. $QRS_{min}[n]$ is much away from the actual QRS complex location. This may be due to the false alarm in the corresponding lead.

This false detection of the concerned lead should be discarded and replaced by the next beat of the corresponding lead to generate the correct QRS complex vector. After this replacement, a new QRS complex vector $\mathbf{R}[n]$ is generated. With this new $\mathbf{R}[n]$, again the fusion process is applied. The complete process is shown in the Algorithm 1.

Algorithm 1: Algorithm for case 4 (i)

1 Initialization:

- 1) $n \rightarrow$ Index for current beat under fusion.
- 2) $k \rightarrow$ Index for detected temporal locations as QRS complex in l^{th} lead ($1 \leq l \leq L$).
- 3) $R(n) \rightarrow$ QRS complex vector for the n^{th} beat.
- 4) $\mathbf{f}[n] \rightarrow$ Sorted value of $R[n]$ in ascending order.
- 5) $\alpha_1[n], \alpha_2[n] \rightarrow$ Generated arrays for n^{th} beat
- 6) $QRS_{min}[n] \rightarrow$ Minimum temporal location in $\mathbf{f}[n]$ for n^{th} cycle.
- 7) $R_l(k) \rightarrow k^{th}$ temporal location belongs to lead l ($k \geq n$).

Condition: $card(\alpha_1[n]) < card(\alpha_2[n])$

$R_l[k] := QRS_{min}[n]$ ▷ Find the lead of minimum temporal location in $R[n]$

while $\alpha_1[n] \neq \alpha_2[n]$ **do**

$R_l(k) = R_l(k+1)$ ▷ Update the next temporal location in l_{th} lead

$\mathbf{f}[n]$: Find as in (10)

$\alpha_1[n]$: Find as in (13)

$\alpha_2[n]$: Find as in (14)

end

$QRS_{loc}[n] = \text{find as in (20)}$

For the depiction of case 4(i), results corresponding to the record I29 of INCART database are shown in Fig 4. This record corresponds to a 41 year old female having Premature Ventricular Complexes (PVCs) and Paroxysmal Ventricular Tachycardia. The QRS complex locations detected by single lead detector is marked on all the L leads of the record I29. The arrays formed by the fusion process is also marked. Since both the arrays formed are not identical as shown in Fig 4. As $\alpha_1[n]$ is less than $\alpha_2[n]$, minimum temporal locations of $\alpha_1[n]$ will be replaced by the next temporal locations of the same lead. The replacement of the beat led to identical arrays. The accurate QRS complex location is estimated using (20), which comes out to be at 8.794s as compared to 8.786s marked by physician with an average localization error of only 0.04s. The false positive detected at 8.335s and 8.327s locations for lead V1 and V2 respectively are ignored by the proposed algorithm. The detected QRS complex is estimated with localization error of 8ms only, which is very close to the observed QRS complex by physician.

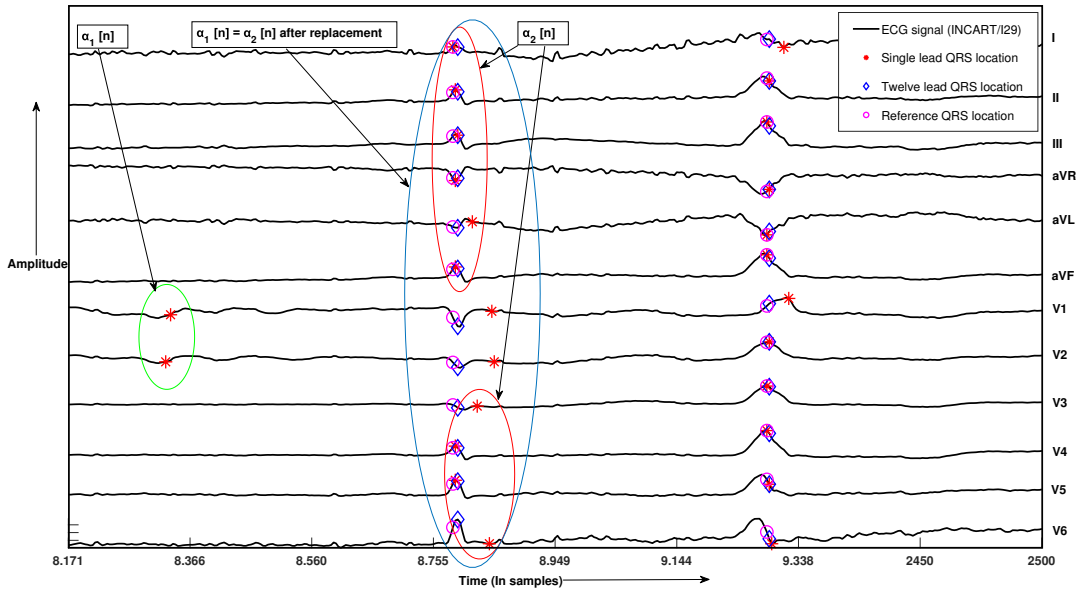


Fig. 4: QRS complex detection by single-lead detector and multi-lead detector in I29 data of INCART database

Case 4(ii): When the cardinality of $\alpha_1[n]$ is more than the cardinality of $\alpha_2[n]$. Here some the detected QRS complex locations corresponding to L leads are much away from $QRS_{max}[n]$ whereas most of them are close to the $QRS_{min}[n]$. This implies that the actual QRS complex location is closer to the array $\alpha_1[n]$ and last few entries of $\alpha_2[n]$ are much away from the actual QRS complex location. There are two possible reasons for this,

- (i) QRS complex detection has been missed for that particular lead and the entry corresponding to the QRS complex belongs to the next cycle. Which should be considered in next cycle.
- (ii) The detected beat may be the tall T wave of present cycle instead of the QRS complex.

In either case fusion algorithm removes corresponding false detected entries from QRS complex vector by ignoring the maximum temporal location of $\alpha_2[n]$. A new QRS complex vector $R[n]$ of reduced length is obtained and the complete fusion process is again applied. These ignored locations are then considered for the beat detection in the next cardiac cycle. This process for case 4 (ii) is also discussed in Algorithm 2.

Algorithm 2: Algorithm for case 4(ii)

1 Initialization:

- 1) $n \rightarrow$ Index for current beat under fusion.
- 2) $q \rightarrow$ Index for QRS complex location in l^{th} lead ($q \geq n + 1$).
- 3) $R(n) \rightarrow$ QRS complex vector for the n^{th} beat.
- 4) $\mathbf{f}[n] \rightarrow$ Sorted value of $R[n]$ in ascending order.
- 5) $\alpha_1[n], \alpha_2[n] \rightarrow$ Generated arrays
- 6) $QRS_{max}[n] \rightarrow$ Maximum temporal location in $\mathbf{f}[n]$.
- 7) $R_l(q) \rightarrow$ QRS location of lead l to be considered in next beat.

Condition: $card(\alpha_1[n]) > card(\alpha_2[n])$

$R_l[q - 1] := QRS_{max}[n]$

\triangleright Find the maximum temporal location in $R[n]$

while $\alpha_1[n] \neq \alpha_2[n]$ **do**

$R_l(q) = R_l(q - 1)$

\triangleright save the $QRS_{max}[n]$ for next cycle

$R_l[q - 1] := \emptyset$

$\mathbf{f}[n]$: Find as in (10)

$\alpha_1[n]$: Find as in (13)

$\alpha_2[n]$: Find as in (14)

end

$QRS_{loc}[n] = \text{find as in (20)}$

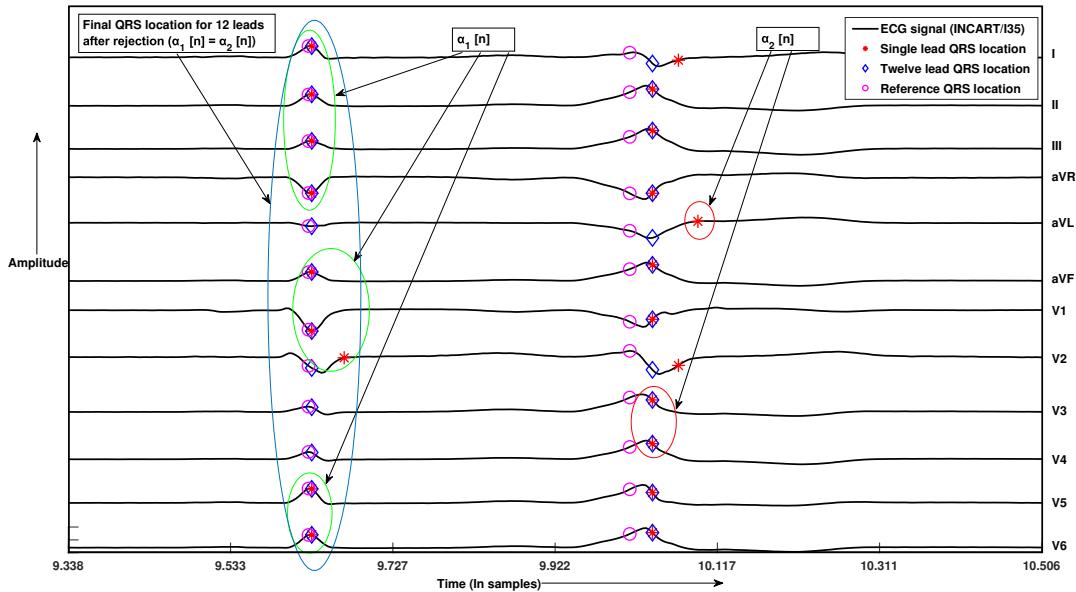


Fig. 5: QRS detection by single-lead detector and multi-lead detector in I35 data of INCART database

For a depiction of case 4(ii), the record I35 of the INCART database is shown in Fig 5. The two arrays generated by the algorithm are shown in Fig 5. In this case, a single lead QRS detector was not able to detect the QRS location in lead aVL, V3, and V4 for the corresponding beat. Therefore the QRS locations of the subsequent beat for these leads is considered by the algorithm. Here the length of $\alpha_2[n]$ is less than the length of $\alpha_1[n]$. The false alarms are ignored until both arrays are identical. The false alarm at the locations 10.093s, 10.039s, and 10.039s for lead aVL, V3, and V4 are ignored. Hence, the accurate QRS complex location is estimated at 9.630s with a localization error of 3.89ms only, which is very close to the observed QRS complex by a physician.

Algorithm 3: Fusion algorithm for the QRS complex detection in 12 lead ECG signals

Input: $R[n], R_{loc}$ \triangleright (Detected QRS location of n^{th} beat in L leads and total QRS temporal locations of L leads)

Output: $\alpha_1[n], \alpha_2[n], QRS_{loc}[n]$ \triangleright (both arrays and final detected QRS location for 12 lead ECG)

1 Function Merge (F) :

2 $\mathbf{f}[n] = \text{sort}(R[n])$;

3 $QRS_{min}[n] \leftarrow$ First temporal location in $\mathbf{f}[n]$;

4 $QRS_{max}[n] \leftarrow$ Last temporal location in $\mathbf{f}[n]$;

5 $\alpha_1[n] =$ Temporal location within δ limit of $QRS_{min}[n]$

6 $\alpha_2[n] =$ Temporal location within δ limit of $QRS_{max}[n]$

7 **while** $\alpha_1[n] \neq \alpha_2[n]$ **do**

8 **if** $\text{card}(\alpha_1[n]) < \text{card}(\alpha_2[n])$ **then**

9 Replace $QRS_{min}[n]$ by next detected temporal location in same lead

10 **else if** $\text{card}(\alpha_1[n]) > \text{card}(\alpha_2[n])$ **then**

11 Ignore $QRS_{max}[n]$ for next cycle

12 **else**

13 Replace $QRS_{min}[n]$ and Ignore $QRS_{max}[n]$

14 **end**

15 **end**

16 $QRS_{loc}[n] =$ median of $\alpha_1[n]$ or $\alpha_2[n]$

17 **End Function**

The complete fusion algorithm for the detection of QRS complex in 12 lead ECG signal is summarized as in Algorithm 3.

III. DATABASE AND EXPERIMENTAL RESULTS

A. ECG databases:

The proposed algorithm is evaluated on the St. Petersburg Institute of Cardiological Technics 12-lead Arrhythmia Database (INCART Database)[1] and the Common Standards for Electrocardiography (CSE) multilead database [2]. The INCART database consist of 75 annotated twelve lead ECG recording of length 30 min, each sampled at 257 Hz. The total number of beat annotation in INCART database are 175,000. The CSE set 3 database consist of 125 records of length 10 second sampled at 500Hz. The CSE multi-lead database have 15 lead simultaneously recorded ECG signals, in which 12 standard leads (I, II, III, aVR, aVL, aVF, V1, V2, V3,V4, V5 and V6) and 3 orthogonal lead(X,Y and Z). Both database have a variety of waveforms with artifacts that an arrhythmia detector might encounter in routine clinical use like sinus node function, coronary artery disease and accute myocardial infarction (MI).

B. Performance evaluation:

The performance of the proposed algorithm is assessed using the following statistical measures as,

Sensitivity: Percentage of true beats that are correctly detected by the algorithm.

$$Se = \frac{TP}{TP + FN} \quad (21)$$

Positive predictivity: Percentage of detected beats that is true beats

$$+Pr = \frac{TP}{TP + FP} \quad (22)$$

Where **TP (true positives):** Actual QRS complex locations detected as QRS Complex,

FN(false negatives): Actual QRS complex locations which have not been detected, and

FP(false positives): non-QRS complex locations detected as QRS complex.

The algorithm's performance is validated through the two standard twelve lead ECG databases, namely St. Petersburg INCART database [1] and CSE database [2]. Initially, the single lead QRS complex detection algorithm is evaluated on 12 leads of the INCART database. The comparative results of average sensitivity and positive predictivity with the reported results in literature [17],

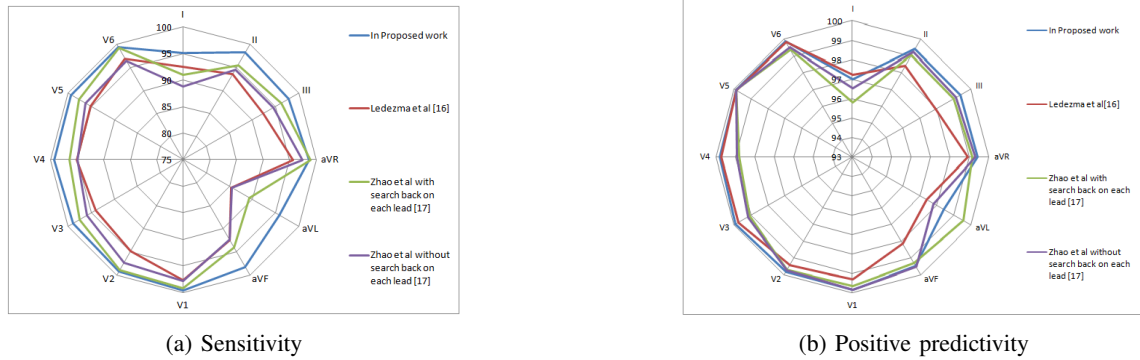


Fig. 6: Performance of single lead QRS detector on 12 lead INCART database

[18] are shown in Fig 6. It can be seen from Fig 6 that the performance of the proposed algorithm presented in this paper is much better as compared to the other methods reported in the literature. The method gives the average sensitivity ($Se\%$) of 99.55% and average positive predictivity ($+Pr\%$) of 99.87% in lead V1, which is higher than the methods reported in the literature for the same number of leads. After obtaining the QRS complex in all L leads independently by a single lead QRS complex detector, the proposed fusion method is applied. As discussed in the fusion method, the median of the all valid QRS complex location, satisfying the fusion condition, is taken instead of the mean to merged the L lead. Experimentally, we observed better results when the median was taken of the L detected beats compared to the mean and mode. The performance of the fusion method on 75 records of the INCART database in terms of sensitivity and positive predictivity for median and mean is shown in Fig 7. It can be seen that results obtained for the median are much better. Even the physicians annotate the QRS complex in the middle of QRS onset, and endpoint [21]. The research work on QRS detection available in literature allows a window up to 320 ms, which exceeds the maximum allowable tolerance (150 ms) for QRS detection accuracy allowed by the ANSI/AAMI-EC38, EC57 standards. The EC38 and EC 57 standards are strictly followed in this work while reporting the results, as the bxb program of the WFDB toolbox is used. The bxb is an ANSI/AAMI-standard beat-by-beat annotation comparator [36], which matched up the detected QRS complex location with reference QRS complex annotations within the tolerance limit. The proposed method gives better performance even after including data I02, I03, I57, and I58 compared

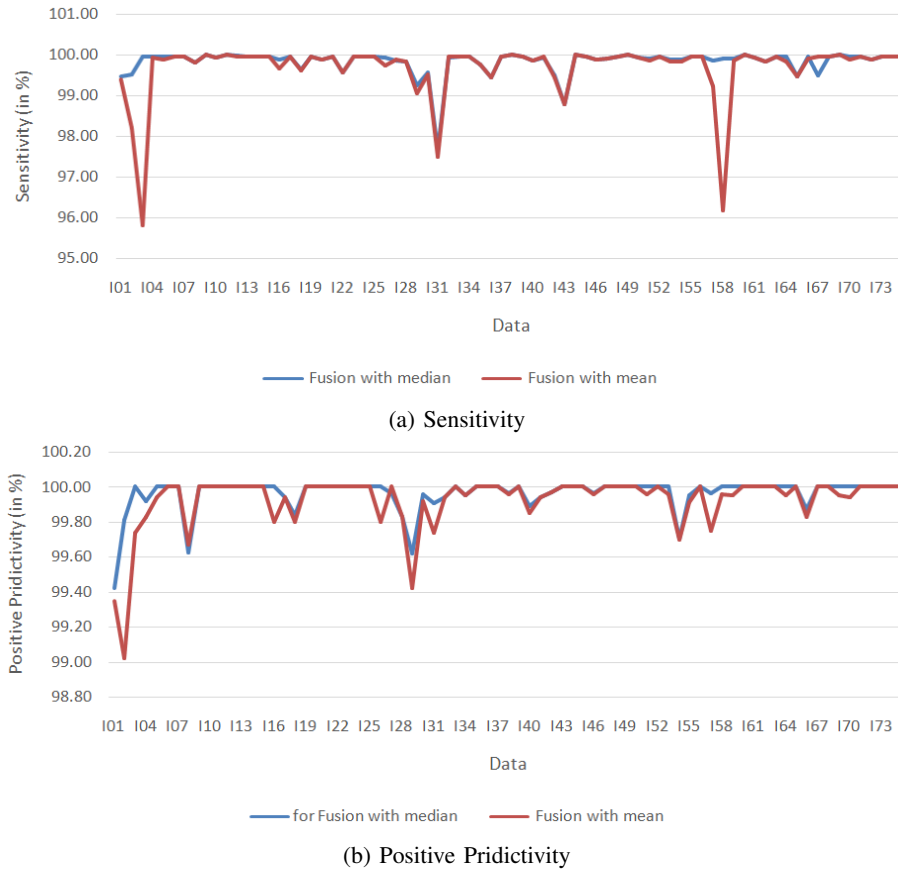


Fig. 7: Comparison of median-fusion and mean-fusion method on INCART database

to other methods with sensitivity ($Se\%$) of 99.87% and positive predictivity ($+Pr\%$) of 99.96% as shown in Table III. Hence, the proposed method works satisfactorily in the absence or low signal in any lead due to bad contact of the electrode. As shown in Fig 8, the tall T waves were detected as QRS complex by a single lead QRS detector, but it was ignored by the proposed twelve lead QRS complex detector. The L lead QRS detector detects the QRS complex locations with 100% sensitivity and positive predictivity by discarding the FP detected by a single lead QRS detector. As 100% sensitivity and positive predictivity of QRS complex detector are required for accurate MI detection, our proposed method gives the desirable results on most of the ECG signals. In Table III, the record I56 of the INCART database corresponds to a 74-year-old male with have earlier MI. The

proposed method detected all the QRS locations with 100% sensitivity and positive predictivity in this case.

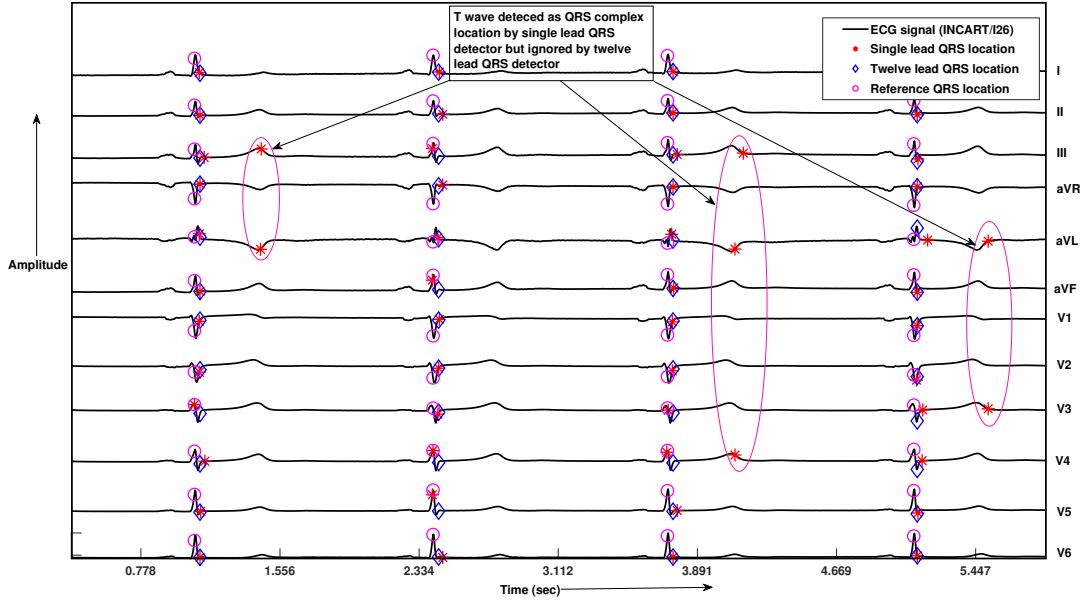


Fig. 8: QRS detection in record I26 of INCART database

The L lead QRS detector is also evaluated on the CSE database. The proposed method gives the sensitivity of 100% and positive predictivity 99.13% on the CSE database, which is better than other methods. It can be seen that the fusion of all leads improves the QRS complex location. In Fig 9, the signal M0_109 of the CSE database is shown, in which the QRS complex locations not detected by [16], [27] are detected by the proposed algorithm. The comparative results of average Sensitivity and Positive Predictivity with the reported results in literature [24], [19], [27], [37], [28], [38], [29], [39] are shown in Table I. Hence, the proposed method shows satisfactory performance on both the databases. The method reported in [19] require a supervised training period to learn the weights of each lead. Therefore it can not be used for short duration ECG recordings of CSE database have 10 sec of duration. The method given by [29] requires the full ECG signal to extract the principle components. Therefore, this can not be used for the real-time medical devices. In contrast, the proposed multi-lead fusion algorithm act as the performance booster of any single lead QRS

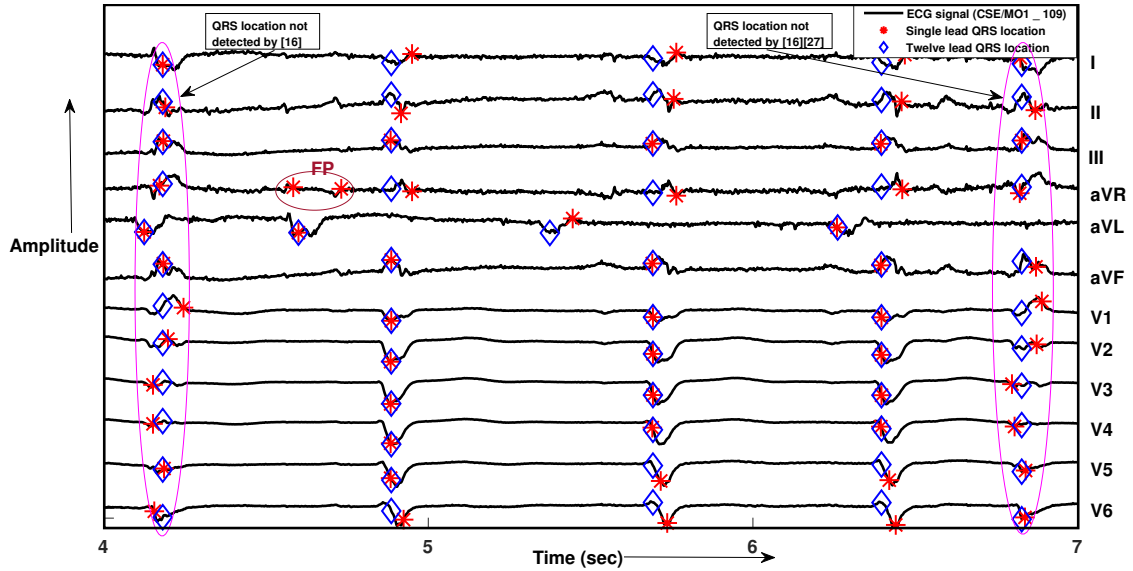


Fig. 9: QRS detection in record *MO1_109* of CSE database

complex detector. Hence, our method is suitable for the automation of a Holter device for real-time monitoring as well as for recorded ECG signal. The proposed algorithm is implemented in MATLAB on a i7 processor. The processing time to detect QRS complex location in 12 lead ECG signals of INCART database is given in Table II.

TABLE I: Comparison of proposed 12 lead QRS complex detector with existing methods

Database	Method	No. of beat	TP	FN	FP	Se	+Pr
INCART	Proposed	175906	175628	278	75	99.87	99.96
	Thurner et al (2021) [24]	N/R*	175130	789	738	99.55	99.58
	Ledezma et al (GQRS)(2019)[19]	147570	147469	101	186	99.94	99.88
	Ledezma et al(PT) (2019)[19]	175906	175738	168	157	99.91	99.92
	Mondelo et al (2017) [28]	≈ 81517	N/R*	N/R*	N/R*	99.86	99.98
	huang et al (2009) [29]	175900	175863	35	6	99.98	99.99
CSE	Proposed	1488	1488	00	13	100	99.13
	Mehta et al (2009)[37]	1488	1484	04	24	99.73	98.40
	Saini et al (2013) [27]	1488	1486	02	02	99.86	99.86
	Vitek et al (2009) [39]	N/R*	N/R*	N/R*	N/R*	99.19	N/R*
	Mehta et al (2007) [38]	1488	1487	01	13	99.93	99.13

* Not Reported

TABLE II: Processing time of the proposed method

S.No.	Algorithms	Processing time (in second)			Duration of ECG recording
		Mean	Variance	Standard deviation	
1	Multi-Lead Fusion	0.6599	0.0933	0.3055	30 min
2	QRS detector and Multi-Lead Fusion	28.3626	0.2266	0.4761	30 min

IV. CONCLUSION

In this paper, a novel multi-lead fusion algorithm is designed for accurate delineation of QRS complex in the 12 lead ECG signal. The proposed algorithm is based on the QRS complex detection of single lead ECG signal. The proposed method is robust against the noise or artifacts present in the ECG signal. The detection is not affected by the change of morphology of the ECG signal. The effectiveness of the proposed method was tested on standard ECG databases like CSE and INCART databases. The detection performance is measured in terms of sensitivity and positive predictivity. The results obtained are compared with the existing detectors in terms of sensitivity and positive predictivity. The proposed algorithm is suitable for automated handheld devices to detect the real-time change in ECG signal. This method can be used for real time processing of huge ECG recorded data over a long period of time and tele-medicine application.

REFERENCES

- [1] A. L. Goldberger, L. A. Amaral, L. Glass, J. M. Hausdorff, P. C. Ivanov, R. G. Mark, J. E. Mietus, G. B. Moody, C.-K. Peng, and H. E. Stanley, "Physiobank, physiotoolkit, and physionet: components of a new research resource for complex physiologic signals," *circulation*, vol. 101, no. 23, pp. e215–e220, 2000.
- [2] J. L. Willems, P. Arnaud, J. H. Van Bommel, P. J. Bourdillon, R. Degani, B. Denis, I. Graham, F. M. Harms, P. W. Macfarlane, G. Mazzocca *et al.*, "A reference data base for multilead electrocardiographic computer measurement programs," *Journal of the American College of Cardiology*, vol. 10, no. 6, pp. 1313–1321, 1987.
- [3] C. Van Mieghem, M. Sabbe, and D. Knockaert, "The clinical value of the ecg in noncardiac conditions," *Chest*, vol. 125, no. 4, pp. 1561–1576, 2004.
- [4] G. Chen, M. Chen, J. Zhang, L. Zhang, and C. Pang, "A crucial wave detection and delineation method for twelve-lead ecg signals," *IEEE Access*, vol. 8, pp. 10 707–10 717, 2020.
- [5] A. Habib, C. Karmakar, and J. Yearwood, "Impact of ecg dataset diversity on generalization of cnn model for detecting qrs complex," *IEEE access*, vol. 7, pp. 93 275–93 285, 2019.
- [6] J. Pan and W. J. Tompkins, "A real-time qrs detection algorithm," *IEEE transactions on biomedical engineering*, no. 3, pp. 230–236, 1985.

- [7] P. S. Hamilton and W. J. Tompkins, "Quantitative investigation of qrs detection rules using the mit/bih arrhythmia database," *IEEE transactions on biomedical engineering*, no. 12, pp. 1157–1165, 1986.
- [8] N. M. Arzeno, Z.-D. Deng, and C.-S. Poon, "Analysis of first-derivative based qrs detection algorithms," *IEEE Transactions on Biomedical Engineering*, vol. 55, no. 2, pp. 478–484, 2008.
- [9] S. Pal and M. Mitra, "Empirical mode decomposition based ecg enhancement and qrs detection," *Computers in biology and medicine*, vol. 42, no. 1, pp. 83–92, 2012.
- [10] P. Sabherwal, M. Agrawal, and L. Singh, "Automatic detection of the r peaks in single-lead ecg signal," *Circuits, Systems, and Signal Processing*, vol. 36, no. 11, pp. 4637–4652, 2017.
- [11] E. A. Junior, R. A. de Medeiros Valentim, and G. B. Brandao, "Real time qrs detection based on redundant discrete wavelet transform," *IEEE Latin America Transactions*, vol. 14, no. 4, pp. 1662–1668, 2016.
- [12] M. Jia, F. Li, J. Wu, Z. Chen, and Y. Pu, "Robust qrs detection using high-resolution wavelet packet decomposition and time-attention convolutional neural network," *IEEE Access*, vol. 8, pp. 16 979–16 988, 2020.
- [13] A. Sharma, S. Patidar, A. Upadhyay, and U. R. Acharya, "Accurate tunable-q wavelet transform based method for qrs complex detection," *Computers & Electrical Engineering*, vol. 75, pp. 101–111, 2019.
- [14] B. S. Chandra, C. S. Sastry, and S. Jana, "Robust heartbeat detection from multimodal data via cnn-based generalizable information fusion," *IEEE Transactions on Biomedical Engineering*, vol. 66, no. 3, pp. 710–717, 2018.
- [15] J. Liu, X. Tan, C. Huang, and X. Ji, "A dual-lead fusion detection algorithm of qrs," in *Third International Conference on Cyberspace Technology (CCT 2015)*, 2015, pp. 1–6.
- [16] P. Laguna, R. Jané, and P. Caminal, "Automatic detection of wave boundaries in multilead ecg signals: Validation with the cse database," *Computers and biomedical research*, vol. 27, no. 1, pp. 4–60, 1994.
- [17] C. A. Ledezma, G. Perpiñan, E. Severeyn, and M. Altuve, "Data fusion for qrs complex detection in multi-lead electrocardiogram recordings," in *11th international symposium on medical information processing and analysis*, vol. 9681. International Society for Optics and Photonics, 2015, p. 968118.
- [18] W. Zhao, Y. Xu, C. Yan, J. Hu, D. Jia, X. Sun, and T. You, "A multilead fusion based qrs complex detection method on 12-lead electrocardiogram signals," in *2018 Computing in Cardiology Conference (CinC)*, vol. 45. IEEE, 2018, pp. 1–4.
- [19] C. A. Ledezma and M. Altuve, "Optimal data fusion for the improvement of qrs complex detection in multi-channel ecg recordings," *Medical & biological engineering & computing*, vol. 57, no. 8, pp. 1673–1681, 2019.
- [20] —, "Fusión de datos para detectar complejos qrs en registros electrocardiográficos multicanal," in *V Congreso Venezolano de Bioingeniería, Mérida, Venezuela*, vol. 162, 2015.
- [21] M. Yochum, C. Renaud, and S. Jacquir, "Automatic detection of p, qrs and t patterns in 12 leads ecg signal based on cwt," *Biomedical signal processing and control*, vol. 25, pp. 46–52, 2016.
- [22] Q. Yu, Q. Guan, P. Li, T.-B. Liu, X.-L. Huang, Y. Zhao, H.-X. Liu, and Y.-Q. Wang, "Fusion of detected multi-channel maternal electrocardiogram (ecg) r-wave peak locations," *Biomedical engineering online*, vol. 15, no. 1, pp. 1–16, 2016.
- [23] S. S. Mehta and N. S. Lingayat, "Combined entropy based method for detection of qrs complexes in 12-lead electrocardiogram using svm," *Computers in biology and medicine*, vol. 38, no. 1, pp. 138–145, 2008.

- [24] T. Thurner, C. Hintermueller, H. Blessberger, and C. Steinwender, "Complex-pan-tompkins-wavelets: Cross-channel ecg beat detection and delineation," *Biomedical Signal Processing and Control*, vol. 66, p. 102450, 2021.
- [25] R. Smíšek, L. Maršánová, A. Němcová, M. Vitek, J. Kozumplík, and M. Nováková, "Cse database: extended annotations and new recommendations for ecg software testing," *Medical & biological engineering & computing*, vol. 55, no. 8, pp. 1473–1482, 2017.
- [26] S. Saxena, V. Kumar, and S. Hamde, "Feature extraction from ecg signals using wavelet transforms for disease diagnostics," *International Journal of Systems Science*, vol. 33, no. 13, pp. 1073–1085, 2002.
- [27] I. Saini, D. Singh, and A. Khosla, "Qrs detection using k-nearest neighbor algorithm (knn) and evaluation on standard ecg databases," *Journal of advanced research*, vol. 4, no. 4, pp. 331–344, 2013.
- [28] V. Mondelo, M. J. Lado, A. J. Méndez, X. A. Vila, and L. Rodríguez-Liñares, "Combining 12-lead ecg information for a beat detection algorithm," *Journal on Advances in Theoretical and Applied Informatics*, vol. 3, no. 1, pp. 5–9, 2017.
- [29] B. Huang and Y. Wang, "Qrs complexes detection by using the principal component analysis and the combined wavelet entropy for 12-lead electrocardiogram signals," in *2009 Ninth IEEE international conference on computer and information technology*, vol. 1. IEEE, 2009, pp. 246–251.
- [30] C. K. Reddy, C. C. Aggarwal, C. Reddy, and C. Aggarwal, "An introduction to healthcare data analytics." 2015.
- [31] E. Castillo, D. P. Morales, A. García, F. Martínez-Martí, L. Parrilla, and A. J. Palma, "Noise suppression in ecg signals through efficient one-step wavelet processing techniques," *Journal of Applied Mathematics*, vol. 2013, 2013.
- [32] R. Polikar *et al.*, "The wavelet tutorial," 1996.
- [33] M. Elgendi, M. Jonkman, and F. De Boer, "R wave detection using coiflets wavelets," in *2009 IEEE 35th Annual Northeast Bioengineering Conference*. IEEE, 2009, pp. 1–2.
- [34] G. Pal and P. Pal, "Textbook of practical physiology. hyderabad," 2013.
- [35] M. Jim Frost, "Introduction to statistics: An intuitive guide for analyzing data and unlocking discoveries," *Statistics by Jim publishing*, 2019.
- [36] I. Silva and G. B. Moody, "An open-source toolbox for analysing and processing physionet databases in matlab and octave," *Journal of open research software*, vol. 2, no. 1, 2014.
- [37] S. S. Mehta and N. S. Lingayat, "Identification of qrs complexes in 12-lead electrocardiogram," *Expert Systems with Applications*, vol. 36, no. 1, pp. 820–828, 2009.
- [38] —, "Development of entropy based algorithm for cardiac beat detection in 12-lead electrocardiogram," *Signal Processing*, vol. 12, no. 87, pp. 3190–3201, 2007.
- [39] M. Vitek, J. Hrubeš, and J. Kozumplík, "A wavelet-based ecg delineation in multilead ecg signals: Evaluation on the cse database," in *World Congress on Medical Physics and Biomedical Engineering, September 7-12, 2009, Munich, Germany*. Springer, 2009, pp. 177–180.

TABLE III: Results of 12 lead QRS detector on INCART Database

Records	Actual QRS	TP	FN	FP	Records	Actual QRS	TP	FN	FP
I01	2757	2742	15	16	I39	1775	1775	0	0
I02	2674	2662	12	5	I40	2666	2663	3	3
I03	2451	2451	0	0	I41	1630	1630	0	1
I04	2424	2424	0	2	I42	3109	3095	14	1
I05	1776	1776	0	0	I43	2209	2183	26	0
I06	2493	2493	0	0	I44	2495	2495	0	0
I07	2706	2706	0	0	I45	1928	1928	0	0
I08	2131	2128	3	8	I46	2658	2656	2	1
I09	2997	2997	0	0	I47	1953	1952	1	0
I10	3682	3680	2	0	I48	2357	2357	0	0
I11	2106	2106	0	0	I49	2147	2147	0	0
I12	2809	2809	0	0	I50	2998	2997	1	0
I13	2023	2023	0	0	I51	2777	2776	1	0
I14	1866	1866	0	0	I52	1747	1747	0	0
I15	2635	2635	0	0	I53	2262	2261	1	0
I16	1522	1521	1	0	I54	2363	2362	1	7
I17	1673	1673	0	1	I55	2166	2166	0	1
I18	3084	3075	9	5	I56	1705	1705	0	0
I19	2063	2063	0	0	I57	2871	2869	2	0
I20	2652	2650	2	0	I58	2325	2324	1	0
I21	2184	2184	0	0	I59	2148	2147	1	0
I22	3126	3113	13	0	I60	2475	2475	0	0
I23	2205	2205	0	0	I61	1454	1454	0	0
I24	2571	2571	0	0	I62	2269	2266	3	0
I25	1712	1712	0	0	I63	1994	1994	0	0
I26	1509	1509	0	0	I64	1913	1913	0	0
I27	2605	2601	4	1	I65	2664	2650	14	0
I28	1717	1715	2	3	I66	2340	2340	0	3
I29	2621	2605	16	10	I67	2975	2960	15	0
I30	2462	2451	11	1	I68	2644	2644	0	0
I31	3210	3138	72	3	I69	2169	2169	0	0
I32	1619	1619	0	1	I70	1666	1666	0	0
I33	1837	1837	0	0	I71	1670	1670	0	0
I34	1965	1965	0	1	I72	2270	2269	1	0
I35	3676	3668	8	0	I73	1992	1992	0	0
I36	3911	3890	21	0	I74	2405	2405	0	0
I37	2461	2461	0	0	I75	2103	2103	0	0
I38	2699	2699	0	1	Total	175906	175628	278	75

TABLE IV: Results of 12 lead QRS detector on CSE Database (prefix MO1_ with each record)

Records	Actual QRS	TP	FN	FP	Records	Actual QRS	TP	FN	FP	Records	Actual QRS	TP	FP	FN
001	11	11	0	0	043	10	10	0	0	085	11	11	0	0
002	19	19	0	0	044	08	08	0	0	086	09	09	0	0
003	17	17	0	0	045	13	13	0	0	087	09	09	0	0
004	16	16	0	0	046	12	12	0	0	088	09	09	0	0
005	17	17	0	0	047	16	16	0	0	089	06	06	1	0
006	16	16	0	0	048	10	10	0	0	090	08	08	0	0
007	17	17	0	0	049	11	11	0	0	091	09	09	0	0
008	10	10	0	0	050	08	08	0	0	092	11	11	0	0
009	12	12	0	0	051	20	20	0	0	093	09	09	0	0
010	07	07	4	0	052	15	15	0	0	094	10	10	0	0
011	15	15	0	0	053	17	17	0	0	095	08	08	0	0
012	13	13	1	0	054	07	07	4	0	096	08	08	0	0
013	12	12	0	0	055	09	09	0	0	097	09	09	1	0
014	08	08	0	0	056	10	10	0	0	098	11	11	0	0
015	06	06	0	0	057	10	10	0	0	099	10	10	0	0
016	16	16	0	0	058	15	15	0	0	100	15	15	0	0
017	10	10	0	0	059	08	08	0	0	101	16	16	0	0
018	15	15	0	0	060	12	12	0	0	102	16	16	0	0
019	13	13	0	0	061	13	13	0	0	103	11	11	0	0
020	22	22	0	0	062	11	11	0	0	104	08	08	0	0
021	07	07	0	0	063	09	09	0	0	105	14	14	0	0
022	12	12	0	0	064	11	11	0	0	106	10	10	0	0
023	08	08	0	0	065	12	12	0	0	107	14	14	0	0
024	09	09	0	0	066	10	10	0	0	108	16	16	0	0
025	10	10	0	0	067	12	12	0	0	109	15	15	0	0
026	13	13	0	0	068	16	16	0	0	110	15	15	0	0
027	14	14	0	0	069	13	13	0	0	111	20	20	0	0
028	10	10	0	0	070	12	12	0	0	112	13	13	0	0
029	10	10	0	0	071	14	14	0	0	113	17	17	0	0
030	12	12	0	0	072	11	11	0	0	114	11	11	0	0
031	13	13	0	0	073	13	13	0	0	115	20	20	0	0
032	14	14	0	0	074	10	10	0	0	116	13	13	0	0
033	09	09	0	0	075	13	13	0	0	117	12	12	0	0
034	12	12	0	0	076	13	13	0	0	118	11	11	0	0
035	11	11	0	0	077	12	12	0	0	119	18	18	0	0
036	12	12	0	0	078	07	07	0	0	120	09	09	0	0
037	13	13	0	0	079	09	09	1	0	121	10	10	0	0
038	11	11	0	0	080	09	09	0	0	122	15	15	0	0
039	09	09	0	0	081	12	13	0	0	123	13	13	0	0
040	12	12	0	0	082	09	09	1	0	124	11	11	0	0
041	11	11	0	0	083	15	15	0	0	125	12	12	0	0
042	11	11	0	0	084	10	10	0	0	Total	1488	1488	13	0